Quantum Mechanical Investigation of the Atmospheric Reaction CH_3O_2 + NO

Antonija Lesar,*,† Milan Hodošček,†,‡ Evangelos Drougas,§ and Agnie M. Kosmas*,§

Department of Physical and Organic Chemistry, Insitute Jožef Stefan, Jamova 39, SI-1000, Ljubljana, Slovenia, Centre for Molecular Modeling, National Institute of Chemistry, Hajdrihova 19, SI-1000, Ljubljana, Slovenia, and Division of Physical Chemistry, Department of Chemistry, University of Ioannina, Greece 45110

Received: March 8, 2006; In Final Form: May 4, 2006

The important stationary points on the potential energy surface of the reaction CH_3O_2 + NO have been investigated using ab initio and density functional theory techniques. The optimizations were carried out at the B3LYP/6-311++G(d,p) and MP2/6-311++G(d,p) levels of theory while the energetics have been refined using the G2MP2, G3//B3LYP, and CCSD(T) methodologies. The calculations allow the proper characterization of the transition state barriers that determine the fate of the nascent association conformeric minima of methyl peroxynitrite. The main products, CH_3O + NO_2, are formed through either rearrangement of the trans-conformer to methyl nitrate and its subsequent dissociation or via the breaking of the peroxy bond of the cis-conformer to CH_3O + NO_2 radical pair. The important consequences of the proposed mechanism are (a) the allowance on energetic grounds for nitrate formation parallel to radical propagation under favorable external conditions and (b) the confirmation of the conformational preference of the homolytic cleavage of the peroxy bond, discussed in previous literature.

Introduction

The reactions of alkylperoxy radicals with nitric oxide[1,2] play a central role in atmospheric chemistry with severe implications on tropospheric ozone concentrations. The major reaction channel (1) leads to radical pair production (alkoxy radical + NO_2) that enhances ozone formation through the intermediate NO_2 photolysis. A second pathway (2) has been persistently examined that terminates the radical chain reaction and produces alkyl nitrates, acting as NO_x reservoir compounds:

$$RO_2 + NO \rightarrow RO + NO_2 \quad (1)$$

$$\rightarrow RONO_2 \quad (2)$$

The pressure and temperature dependence of the branching ratio of the nitrate formation channel and the effect of the substitution with electron-withdrawing and electron-donating groups upon the branching ratio and the overall rate constant have been the subject of numerous experimental studies.[3−18] They have also motivated several theoretical investigations of the intermediate complexes and the mechanism of these reactions.[19−24]

The important conclusion of the experimental studies is that reaction 2 may account for the observation of small concentrations of alkyl nitrates in the troposphere at low-temperature and high-pressure conditions, produced through a low barrier isomerization of the association alkylperoxy nitrite intermediate to the nitrate form. The mechanism of the reaction for example, between methylperoxy radicals and nitrogen monoxide has been suggested to involve the formation of the nascent association methylperoxy nitrite minimum in two distinct conformeric structures, the *cis*-perp and the *trans*-perp forms, that proceed further to reaction products, i.e., either the radical pair formation, CH_3O + NO_2, or the methyl nitrate production, CH_3ONO_2. The controversial issue that has complicated the formulation of a quantitative mechanism has been the accurate determination of the activation barriers for the various intervening steps, i.e, the cis−trans interconversion and the peroxy, −OONO, to nitrate, $-ONO_2$, isomerization, as well as the barriers for the radical pair CH_3O + NO_2 production. It has been by now well realized that B3LYP/6-311G++(d,p) and MP2/6-311G++(d,p) optimizations produce unrealistically high barriers for the processes under consideration.[19−24] Consequently, they fail to provide reliable critical energy results for the calculation of the branching ratio of nitrate formation, while the modeling of the kinetics of the reactions between various alkylperoxy radicals and NO, tested several times with various parametric schemes, has been shown to require the use of much lower barrier values.[20−22] More specifically, Barker and et.[19,20] have employed master equation models that have been made to reproduce the experimental data for CH_3O_2 + NO_2, provided the activation barriers involved remained below the reactants energy level. Zhang et al.[21] have also confirmed that the fitting of the experimental data for various alkylperoxy radical + NO reactions requires low transition states below both reactant and product radical-pair energies and have suggested the participation of two conformeric structures of peroxy nitrite species in the mechanism of nitrate formation. Finally, Zhao et al.[22] using the CBS-QB3 level of theory were able to detect an interesting conformational preference for the homolytic cleavage of the peroxy bond, by computing a lower barrier for the dissociation of *cis*-peroxy nitrite to radical pair formation than for *trans*-peroxy nitrite. Their theoretical findings for a favored O−O peroxy bond cleavage in the *cis*- rather than in the *trans*-CH_3OONO conformer were paralleled with the matching of the structural

* Corresponding authors.
† Insitute Jožef Stefan.
‡ National Institute of Chemistry.
§ University of Ioannina.

10.1021/jp0614244 CCC: $33.50
Published on Web 06/03/2006 PAGE EST: 5.4

characteristics of the resulting $-NO_2$ fragment with the $^2A_1$ ground and $^2B_2$ excited electronic states of free NO_2, respectively.

In this work we have examined the most important stationary points in the potential energy surface of the $CH_3O_2 + NO$ reaction, considering in detail all possible channels through both nascent association *cis*- and *trans*-peroxy nitrite minima and using a variety of high-level ab initio techniques to secure a reliable description of the energetics of the reaction. The calculations of all the different dissociation channels succeed to incorporate and unify many mechanistic aspects presented in previous literature and to confirm the important role played by the two conformeric minima of methylperoxy nitrite in the overall mechanism of the reaction.[22]

Computational Details

The calculations have been performed using ab initio and density functional theory techniques, namely the (U)MP2[25,26] and the (U)B3LYP[27,28] methods combined with the 6-311++G(d,p) basis set. Minima and transition states were fully optimized and characterized by harmonic vibrational frequency analysis. Intrinsic reaction coordinate (IRC)[29] calculations were used to follow the reaction path in both directions from transition states, to the corresponding reactant and product structures. For stable adducts, anharmonic frequencies were evaluated at the more economical B3LYP level. The energetics have been further refined by employing G2(MP2), G3//B3LYP, and single point CCSD(T) calculations[30,31] on the basis of the B3LYP and MP2 optimized geometries.

All calculations have been carried out with the use of the Gaussian 03 series of programs.[32]

Results and Discussion

The optimized structures of stable isomers and transition states are depicted in Figures 1 and 2, respectively, where it is readily seen that both optimization procedures, MP2 and B3LYP, provide consistent results. The zero-point energy corrected relative energetics are summarized in Table 1 while Figure 3 displays the calculated energy profile.

Deviations between the CCSD(T) and the G2MP2 and G3 relative energetics results are observed in Table 1. The largest discrepancy amounts to 7.4 and 6.3 kcal mol^{-1} for the G2MP2 and the G3 values, respectively. However, the differences observed do not affect the energy order and the mechanism suggested. Differences between CCSD(T) and G2 calculations have been obtained in other cases as well, for instance in the study of the $ClBrO_2$ system.[33]

The discussion on geometrical parameters is based on the MP2 data.

Energy Minima and Isomerization Barriers. As mentioned, three stable minima may be located in the potential energy surface in the reaction $CH_3O_2 + NO$: The methyl nitrate isomer, CH_3ONO_2, and the two nascent association complexes, $CH_3OONOcp$ and $CH_3OONOtp$, i.e., the two conformations of methylperoxy nitrite, characterized by the two dihedral angles, τ(OONO) and τ(COON), equal to 0 and 90° for the *cis*-perp conformer and to 180 and 90° for the *trans*-perp conformer. Their structures have been explored in previous studies, and our findings are in excellent agreement with the literature results.[22−24] The relative stability of the *cis*-perp conformer compared to the *trans*-perp form is found to be about 1.5 kcal mol^{-1} at all levels of theory employed, also in good agreement with the literature findings.[22] The most stable minimum, methyl nitrate, is located at 47.5−53.8 kcal mol^{-1} below reactants

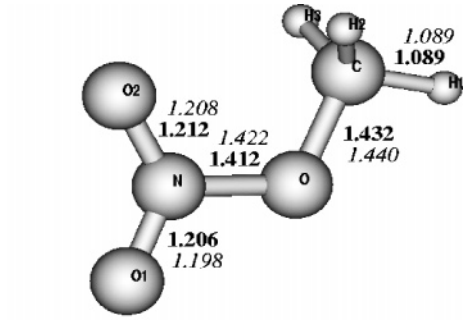

CH_3ONO_2

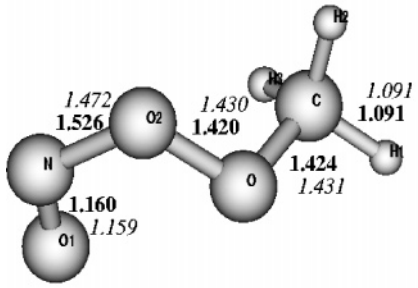

$CH_3OONOcp$

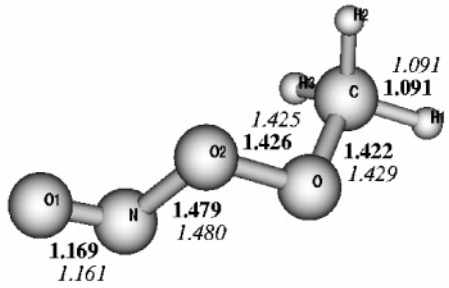

$CH_3OONOtp$

Figure 1. Equilibrium structures of stable isomers. Selected MP2 (bold numbers) and B3LYP (italic numbers) bond lengths (Å) are given; a complete list of parameters is presented in Table S1 of the Supporting Information.

depending on the method employed for the energetics and considerably lower than the $CH_3OONOcp$ conformer by 26.5 kcal mol^{-1} at the CCSD(T)//MP2 level and 29.2 kcal mol^{-1} at the G3//B3LYP level.

Very important features in the potential energy surface are the transition states for the *cis*-perp to *trans*-perp peroxy nitrite rearrangement and the *trans*-perp peroxy nitrite to nitrate isomerization, denoted hereafter as TS*cp-tp* and TS*ono-no*$_2$, respectively. The conformational barrier structure, TS*cp-tp*, has been described in detail by Zhao et al.[22] The associated barrier is found to be located at 10.3, 12.6, 11.0, 12.8, and 12.2 kcal mol^{-1} higher than $CH_3OONOcp$ at the MP2, B3LYP, CCSD(T), G2MP2, and G3//B3LYP levels of theory, also in excellent agreement with Zhao et al.[22] evaluation of 11 kcal mol^{-1} at the UCCSD(T)/6-31+G* level. This value, although lower than the reactant energy level, represents a significant critical energy that does affect the feasibility of the conformational isomerization between the *trans*- and *cis*-peroxy nitrites compared to the other reactions open to each conformer, as we shall see below.

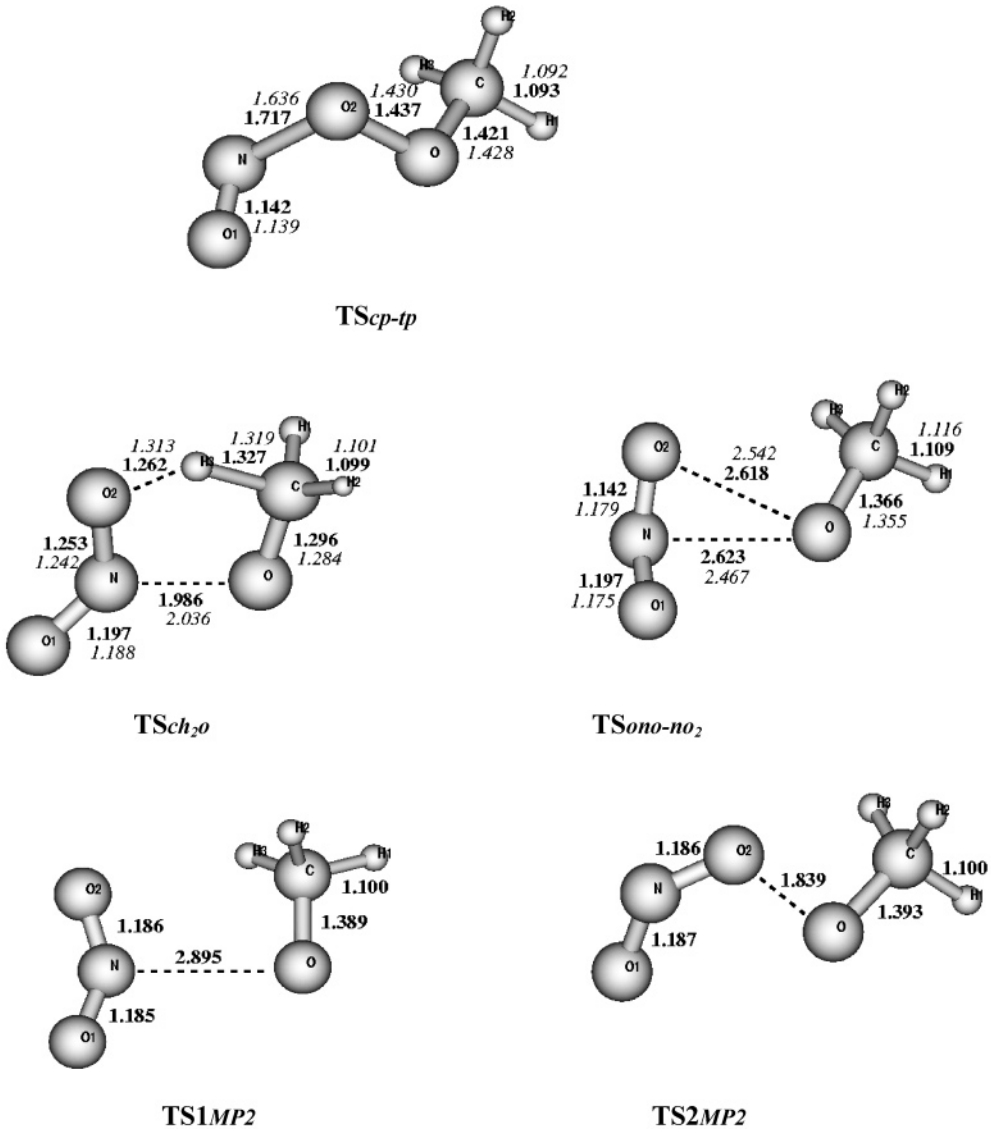

Figure 2. Optimized structures of transition states. Selected MP2 (bold numbers) and B3LYP (italic numbers) bond lengths (Å) are given; a complete list of parameters is presented in Table S2 of the Supporting Information.

TABLE 1: Zero-Point Energy Corrected Relative Energies, ΔE (kcal mol^{-1})[a]

species	MP2	B3LYP	CCSD(T)//[b]MP2	G2MP2	G3//B3LYP
CH_3O_2 + NO	0.0	0.0	0.0	0.0	0.0
CH_3ONO_2	−64.8	−47.7	−47.5	−54.9	−53.8
CH_3OONO*cp*	−30.4	−17.8	−21.0	−26.3	−24.6
CH_3OONO*tp*	−28.9	−16.6	−19.6	−24.9	−23.2
TS*cp-tp*	−20.1	−5.2	−10.0	−13.5	−12.4
TS*ono-no₂*	6.6	15.2	−4.8	−8.9	−8.2
TS*ch₂*o	−24.0	−9.7	−6.6	−12.1	−10.5
TS1*MP2*		−28.5	−9.2		
TS2*MP2*	−17.2	−12.3			
CH_3O + NO_2	−22.0	−15.7	−11.7	−10.6	−12.4
CH_2O + HONO*t*	−82.2	−65.2	−70.0	−72.1	−70.4

[a] CCSD(T)/6-311++G(d,p)//MP2/6-311++G(d,p) calculations.

The isomerization barrier TS*ono-no₂* represents the conversion of CH_3OONO*tp* to methyl nitrate. It results from the substantial elongation of the peroxy bond by 1.192 Å and the simultaneous approach of N atom to the carbon connected O atom to form a triangular geometry with the N−O forming bond to be 2.623 Å. The tension associated with the triangular geometry places this transition state considerably high. The optimization calculations at the MP2 and B3LYP levels locate TS*ono-no₂* at 35.5 and 31.8 kcal mol^{-1}, respectively, higher than CH_3OONO*tp*, i.e., higher than the reactants CH_3O_2 + NO by 6.6 and 15.2 kcal mol^{-1}. This is a result that has been reported in the literature and has created an erroneous impression about the questionable role of the CH_3OONO*tp* ↔ CH_3ONO_2 isomerization channel in the mechanism of the overall reaction. However, the higher level methods, as seen in Table 1, decrease dramatically the magnitude of the isomerization barrier and they place TS*ono-no₂* only 14.8 kcal mol^{-1} at the CCSD(T)//MP2 level and 15.0 kcal mol^{-1} at the G3//B3LYP level higher than CH_3OONO*tp*.

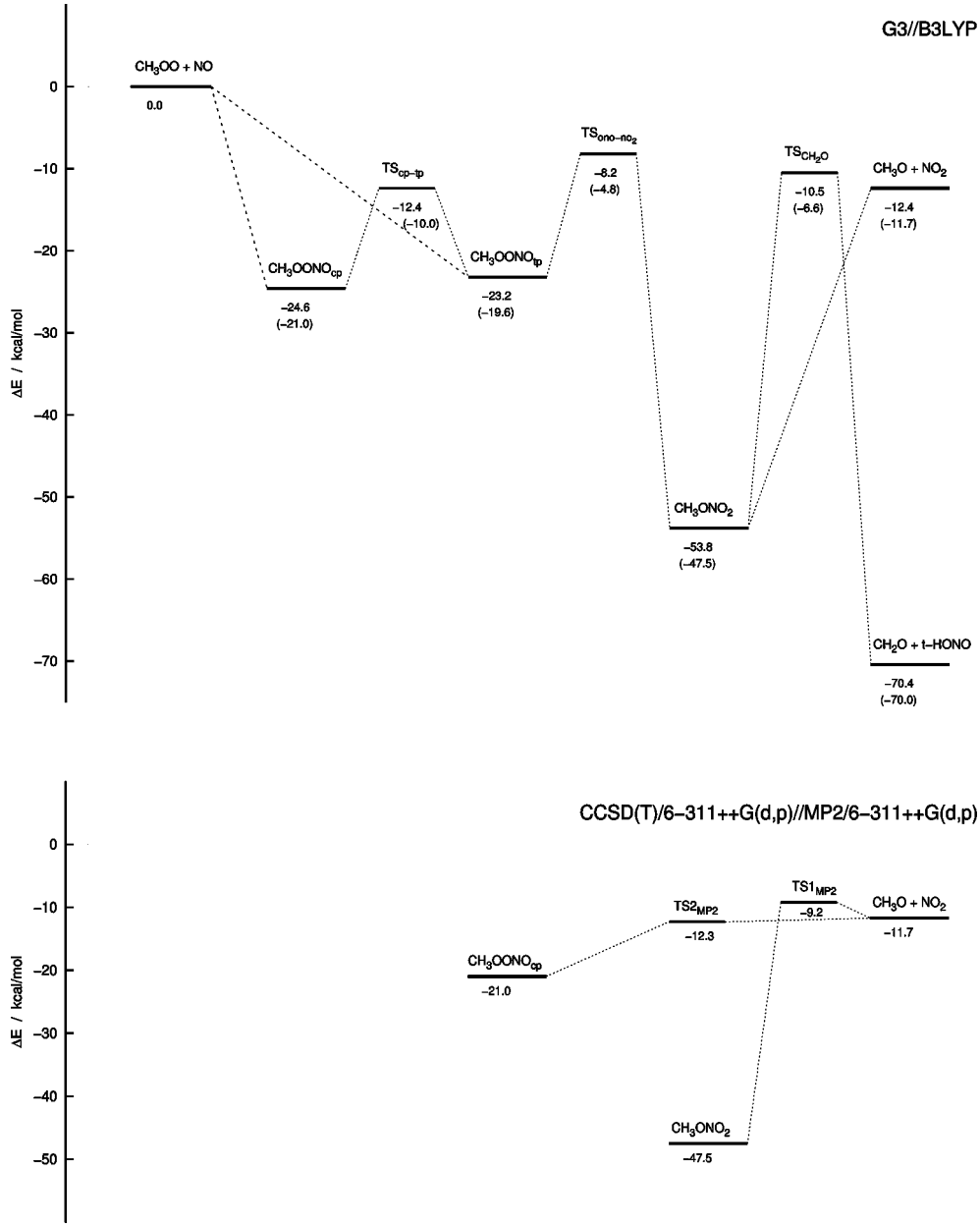

Figure 3. Overall energy profile calculated at the G3//B3LYP level of theory, with the CCSD(T)//MP2 values in parentheses (top panel) and the CH_3OONO*cp* and CH_3ONO_2 decomposition channels at the CCSD(T)//MP2 level of theory (bottom panel).

Thus, the transition state for the *trans*-perp methyl peroxy nitrite ↔ methyl nitrate isomerization is lower located than the reactants by 4.8 kcal mol^{-1} at the CCSD(T)//MP2 level and 8.2 kcal mol^{-1} at the G3//B3LYP level, in excellent agreement with the range of the critical energy values employed for the successful modeling of methyl nitrate yields.[20,21] Consequently, whenever stabilization of CH_3ONO_2 is possible at the low-pressure region, the CH_3OONO*tp* ↔ CH_3ONO_2 isomerization channel provides a good mechanism that explains the formation of small amounts of methyl nitrate detected in the troposphere.

Reaction Pathways for the CH_3OONO*tp* Conformer. It is clear from the reaction profile depicted in Figure 3 that the two conformers once formed behave differently and follow different production pathways. The *trans*-perp conformer isomerizes through the TS*ono-no*$_2$ isomerization transition state discussed above, to methyl nitrate that can be stabilized under favorable temperature and pressure conditions and act as a reservoir species for NO_x.

More frequently, the activated CH_3ONO_2 will dissociate through the transition state TS1*MP2* to radical pair formation CH_3O + NO_2 that consist the main products of the reaction. Optimization of TS1*MP2* has been achieved using the MP2/6-311++G(d,p) procedure, and the calculated imaginary harmonic frequency of 204i cm^{-1} indicates that it is a first-order saddle point. It is located at 2.5 kcal mol^{-1} higher than the products CH_3O + NO_2 at the CCSD(T) level, and thus, it does pose a small barrier for activated methyl nitrate dissociation although it lies lower than the reactants CH_3O_2 + NO energy level. TS1*MP2* really represents the unstable conformation in the course of the reaction between methoxy radical and NO_2, formed through the approach of the N atom to the methoxy O atom, and shows large analogies with the loose transition state adduct between OH and NO_2, determined by Dixon et al.[34] for $HONO_2$ formation in the study of peroxynitrous acid. Here too the two radicals CH_3O and NO_2 are weakly bound with the equilibrium distance of the N−O bond at 2.895 Å, so that the

process can be considered a fully dissociative one. The energy required to form the $CH_3O + NO_2$ products is quite high relative to CH_3ONO_2, 35.8 and 41.4 kcal mol^{-1} at the CCSD(T)//MP2 and G3//B3LYP levels of theory, respectively.

Another reaction pathway available in principle for activated CH_3ONO_2 is decomposition to $CH_2O + HONO_t$ products. This process may take place via a planar five-member ring transition state, denoted TS*ch*$_2$o, that results from the substantial elongation of the O−N bond by 0.574 Å compared to CH_3ONO_2 and the simultaneous migration of a methylic hydrogen to one of the nitrogen-bonded oxygen atoms O1 or O2. The forming O2−H bond distance decreases to 1.262 Å, and the migrating H atom−carbon atom bond length increases to 1.327 Å. The normal mode associated with the reaction coordinate is found to possess a harmonic frequency of 1491i cm^{-1}. TS*ch*$_2$o is located at 40.8, 38.0, 40.9, 42.8, and 43.3 kcal mol^{-1} higher than CH_3ONO_2 at the MP2, B3LYP, CCSD(T), G2(MP2), and G3//B3LYP levels of theory, respectively, but it always remains lower than the reactants energy. The exothermicity of the process amounts to 22.5, 17.2, and 16.6 kcal mol^{-1} at the CCSD(T), G2(MP2), and G3//B3LYP levels of theory. Comparison of the two reaction channels open to dissociation of activated CH_3ONO_2 indicates that the critical energy required for $CH_2O + HONO_t$ formation is higher than TS1*MP2* by only 2.6 kcal mol^{-1} at the CCSD(T) level. Taking also into account the large exothermicity of this channel, we conclude that there must be a nonnegligible probability for $CH_2O + HONO_t$ production. However, dissociation to radical pair CH_3O+NO_2 is clearly more probable.

Reaction Pathways for the CH_3OONO*cp* Conformer. Two reaction pathways are also open for the dissociation of the *cis*-perp methyperoxy conformer. One pathway already discussed represents the isomerization to *trans*-perp conformer through TS*cp-tp*, which will further follow the fate of the *trans*-perp methylperoxy nitrite isomer, discussed previously. The second important channel involves the breaking of the peroxy bond through the transition state TS2*MP2*, leading directly to the radical pair $CH_3O + NO_2$ formation. TS2*MP2* like TS1*MP2* has been determined only at the MP2/6-311++G(d,p) level, and it also represents a loose structure between CH_3O and NO_2 through the approach of one of the oxygen atoms of the NO_2 radical to the oxygen end of the methoxy species at 1.839 Å. The calculated imaginary frequency of 729i cm^{-1} characterizes this structure as a first-order saddle point, and the CCSD(T) energy locates this transition state at about the same level as the $CH_3O + NO_2$ products, at ~0.6 kcal mol^{-1} below, while the decomposition process is endothermic by 9.3 kcal mol $^{-1}$ at the CCSD(T) level of calculations. The transition state TS2*MP2* is entirely analogous to structure 12 determined by Zhao et al.,[22] although it is found to lie even lower in energy in the present CCSD(T) calculations and at about the same level as the dissociation products, $CH_3O + NO_2$. Thus, this reaction channel that represents the lowest energy pathway describes satisfactorily the main direction of the reaction toward the formation of the radical pair $CH_3O + NO_2$ and reconfirms the conformation-dependent homolytic dissociation of methyl peroxynitrite.

Summary of Overall Mechanism. From the present ab initio and density functional calculations the following features emerge about the overall mechanism of the reaction of methylperoxy radicals with NO. The two distinct conformers of the CH_3OONO intermediate that are assumingly formed with about equal statistically branching ratios exhibit a quite separate chemical behavior and reactivity since the interconversion between the two species is rather slow compared to the other reactions open to each conformer. This is due to three factors: the considerable conformational barrier calculated, the direct homolytic dissociation of the *cis*-perp isomer to form the products $CH_3O + NO_2$, and the severe lowering of the barrier associated with the isomerization of the trans-conformer to the nitrate isomer. Two independent pathways (3) and (4) are thus, found to be the important reaction channels, both leading mainly to the $CH_3O + NO_2$ radial pair production

$$CH_3O_2 + NO \rightarrow CH_3OONOtp \rightarrow TSono\text{-}no_2 \rightarrow CH_3ONO_2 \rightarrow TS1MP2 \rightarrow CH_3O + NO_2 \quad (3)$$

and

$$CH_3O_2 + NO \rightarrow CH_3OONOcp \rightarrow TS2MP2 \rightarrow CH_3O + NO_2 \quad (4)$$

Channel (4) has been discussed already by Zhao et al.[22] Channel (3), however, results from the present CCSD(T), G2MP2, and G3//B3LYP energy calculations that have substantially reduced the isomerization barrier TS*ono-no*$_2$ to around 15 kcal mol^{-1} only, i.e., well below the reactant energy and contrary to the B3LYP and MP2 values. Consequently, production of methyl nitrate is suggested to occur through the *trans*-perp peroxy nitrite isomerization, channel (3), if stabilization under suitable temperature and pressure conditions is possible. More often, methyl nitrate will decompose into $CH_3O + NO_2$. Decomposition of CH_3ONO_2 into $CH_2O + HONO_t$ through a methylic hydrogen migration from the carbon atom to the oxygen atoms O1 or O2 and the breaking of the N−O bond is rather unlikely since it is hindered by a energy barrier larger than the decomposition to $CH_3O + NO_2$.

In summary, the present calculations describe in detail how one conformer connects directly to the radical products, while the other connects to both nitrates and radical products, providing a quantitative mechanism that explains the detection of trace quantities of methyl nitrate in the atmosphere. The barriers determined for each step are entirely consistent with the values used in the parametric schemes employed for the successful modeling of nitrate yields.[20,21]

Acknowledgment. This work was funded in part by the Ministry of Higher Education, Science, and Technology of Slovenia, program Grant No. P2-0148, and in part by the General Secretariat for Research and Technology of Greece, program Grant No. 61/1864. We are grateful for their support.

Supporting Information Available: Optimized structures and harmonic frequencies for all species discussed. This material is available free of charge via the Internet at http://pubs.acs.org.

References and Notes

(1) Wallington, T. J.; Nielsen, O. J.; Sehested, J. Reactions of Organic Peroxy Radicals in the Gas Phase. In *Peroxy Radicals*; Alfassi, Ed.; Wiley & Sons: New York, 1997.

(2) King, M. D.; Thompson, K. C. *Atmos. Environ.* **2003**, *37*, 4517.

(3) Simonaitis, R.; Heicklen, J. *J. Phys. Chem.* **1981**, *85*, 2946.

(4) Plumb, I. C.; Ryan, K. R.; Steven, J. R.; Mulcahy, M. F. R. *J. Phys. Chem.* **1981**, *85*, 3136.

(5) Ravishankara, A. R.; Eisele, F. L.; Kreutter, N. M.; Wine, P. H. *J. Chem. Phys.* **1981**, *74*, 2267.

(6) Zellner, R.; Fritz, B.; Lorennz, K. *J. Atmos. Chem.* **1986**, *4*, 241.

(7) Atkinson, R.; Aschmann, S. M.; Winer, A. M. *J. Atmos. Chem.* **1987**, *5*, 91.

(8) Sehested, J.; Nielsen, O. J.; Wallington, T. J. *Chem. Phys. Lett.* **1993**, *213*, 457.

(9) Masaki, A.; Tsunashima, S.; Washida, N. *Chem. Phys. Lett*. **1994**, *218*, 523.
(10) Villalta, P. W.; Huey, L. G.; Howard, C. J. *J. Phys. Chem*. **1995**, *99*, 12829.
(11) Helleis, F.; Moortgat, G. K.; Crowley, J. N. *J. Phys. Chem*. **1996**, *100*, 17846.
(12) Eberhard, J.; Howard, C. J. *J. Phys. Chem. A* **1997**, *101*, 3360.
(13) Scholtens, K. W.; Messer, B. M.; Cappa, C. D.; Elrod, M. J. *J. Phys. Chem. A* **1999**, *103*, 4378.
(14) Wollenhaupt, M.; Crowley, J. N. *J. Phys. Chem. A* **2000**, *104*, 6429.
(15) Arey, J.; Aschmann, S. K.; Kwok, E. S. E.; Atkinson, R. *J. Phys. Chem. A* **2001**, *105*, 1020.
(16) Xing, J.-H.; Nagai, Y.; Kusuhara, M.; Miyoshi, A. *J. Phys. Chem. A* **2004**, *108*, 10458.
(17) Bacak, A.; Bardwell, M. W.; Raventos, M. T.; Percival, C. J.; Sanchez-Reyna, G.; Shallcross, D. E. *J. Phys. Chem. A* **2004**, *108*, 10681.
(18) Xing, J.-H.; Miyoshi, A. *J. Phys. Chem. A* **2005**, *109*, 4095.
(19) Lohr, L. L.; Barker, J. R.; Shroll, R. M. *J. Phys. Chem. A* **2003**, *107*, 7429.
(20) Barker, J. R.; Lohr, L. L.; Shroll, R. M.; Reading, S. *J. Phys. Chem. A* **2003**, *107*, 7434.
(21) Zhang, J.; Dransfield, T.; Donahue, N. M. *J. Phys. Chem. A* **2004**, *108*, 9082.
(22) Zhao, Y.; Houk, K. N.; Olson, L. P. *J. Phys. Chem. A* **2004**, *108*, 5864.
(23) Pan, X. M.; Fu, Z.; Li, Z. S.; Sun, C. C.; Sun, H.; Su, Z. M.; Wang, R. S. *Chem. Phys. Lett.* **2005**, *409*, 98.
(24) Cheng, X.; Zhou, Z.; Zhao, Y.; Sun, Y.; Zhu, Y. *J. Mol. Struct. THEOCHEM* **2005**, *725*, 103.
(25) Møller, C.; Plesset, M. S. *Phys. Rev.* **1934**, *46*, 618.
(26) Frisch, M. J.; Head-Gordon, M.; Pople, J. A. *Chem. Phys. Lett*. **1990**, *166*, 281.
(27) Becke, A. D. *J. Chem. Phys*. **1993**, *98*, 5648.
(28) Lee, C.; Yang, W.; Parr, R. G. *Phys. Rev.* **1988**, *37*, 785.
(29) Gonzales, C.; Schlegel, H. B. *J. Chem. Phys.* **1989**, *90*, 2154.
(30) Hehre, W. J.; Radom, L.; Schleyer, P.v. R.; Pople, A. J. *Ab initio Molecular Orbital Theory*; Wiley-Interscience: New York, 1986.
(31) Pople, J. A.; Gordon, M. H.; Ragavashari, K. *J. Chem. Phys*. **1987**, *87*, 5968.
(32) Frisch, M. J.; Trucks, G. W.; Schlegel, H. B.; Scuseria, G. E.; Robb, M. A.; Cheeseman, J. R.; Montgomery, J. A., Jr.; Vreven, T.; Kudin, K. N.; Burant, J. C.; Millam, J. M.; Iyengar, S. S.; Tomasi, J.; Barone, V.; Mennucci, B.; Cossi, M.; Scalmani, G.; Rega, N.; Petersson, G. A.; Nakatsuji, H.; Hada, M.; Ehara, M.; Toyota, K.; Fukuda, R.; Hasegawa, J.; Ishida, M.; Nakajima, T.; Honda, Y.; Kitao, O.; Nakai, H.; Klene, M.; Li, X.; Knox, J. E.; Hratchian, H. P.; Cross, J. B.; Bakken, V.; Adamo, C.; Jaramillo, J.; Gomperts, R.; Stratmann, R. E.; Yazyev, O.; Austin, A. J.; Cammi, R.; Pomelli, C.; Ochterski, J.; Ayala, P. Y.; Cui, Q.; Morokuma, K.; Voth, G. A.; Salvador, P.; Dannenberg, J. J.; Zakrzewski, V. G.; Dapprich, S.; Daniels, A. D.; Strain, M. C.; Farkas, O.; Malick, D. K.; Rabuck, A. D.; Raghavachari, K.; Foresman, J. B.; Ortiz, J. V.; Cui, Q.; Baboul, A.; Clifford, S.; Cioslowski, J.; Stefanov, B. B.; Liu, G.; Liashenko, A.; Piskorz, P.; Komaromi, I.; Martin, R. L.; Fox, D. J.; Keith, T.; Al-Laham, M. A.; Peng, C. Y.; Nanayakkara, A.; Challacombe, M.; Gill, P. M. W.; Johnson, B.; Chen, W.; Wong, J. L.; Gonzalez, C.; Pople, J. A. *Gaussian 03*; Gaussian Inc.: Wallingford, CT, 2004.
(33) Guha, S.; Francisco, J. S. *J. Phys. Chem. A* **1997**, *101*, 5347.
(34) Dixon, D. A.; Feller, D.; Zhan, C.-G.; Francisco, J. S. *J. Phys. Chem. A* **2002**, *106*, 3191.